A study of the aerodynamic properties of cotton fiber in the confusor tube of a rotor spinning machine

Sherzod Korabayev[1,2,*], *Husanhon* Bobojanov[2], *Jakhongir* Soloxiddinov[2], *Muhammad* Sadikov[2], *Alijon* Yusupov[2], and *Jamoliddin* Mirzaboev[2]

[1]Namangan Institute of Engineering and Technology, Namangan, Uzbekistan
[2]Namangan institute of textile industry, Namangan, Uzbekistan

Abstract. In this article, the movement of fibers in the air channel and the rotor in the rotor spinning machine was studied. In the experimental work, the uniformity and stability of the velocity field of each channel for moving fibers in an aerodynamic device were checked. In this case, the airflow speed was changed from 5 m/s to 30 m/s. Also, differential equations of motion along the OX and OY axes were created taking into account the air resistance. When determining the movement of fibers in a conical channel, the total speed was divided into components, constant values were found, and general equations of motion were derived.

1 Introduction

The high operational properties of sewing products are inextricably linked to the warp and weft yarns of the fabric that makes up it. The smooth appearance of the yarns, uniformity of thickness along the entire length, and orderly distribution of piles ensure the quality of this product. The fabric is affected by surface, axial, and point-shaped external forces. Due to constant or periodic forces, the external integrity of the yarns changes. The sliding and stretching fibers in the spun yarn greatly affect the product's resistance to longitudinal and transverse forces. One of the urgent issues is to improve the strength property index of fibers by spinning them into yarn. According to the information presented in the scientific literature, there are three different opinions about the strength of a single yarn: the strength of the yarn is made up of the resistance of the fibers to mutual sliding, the breaking of the fibers in the section of the yarn, that is, the sum of the strength of the broken fibers and the resistance to sliding finds. The pneumomechanical spinning process includes the opening and cleaning of cotton wool during opening-cleaning and carding. To get the final yarn product, more carding, cleaning, and stretching are done using a drafting machine and rotor spinning machine. In a rotor spinning machine, the input product is a drafting sliver, which is guided by a feed roller and separated into individual fibers by an opening roller. The separated fibers are separated from the opening roller by air suction along the fiber transport channel. To have satisfactory properties of the yarn and not clog the rotor spinning machine, the supplied sliver

* Corresponding author: sherzod.korabayev@gmail.com

must be free of foreign impurities and hooked fibers. After the fiber is cleaned, it should be twisted. A pneumomechanical yarn creates a twist as it moves through each revolution [1, 2].

Although rotor-spinning machines differ in their structural structure, there are not many differences in their technological structures [3]. The main technological processes carried out in machines of all types and models are almost the same: supply, discretization, transfer of fibers to the spinning chamber (rotor), joining of fibers to form a fiber layer, twisting it into yarn, and winding the yarn. Inside the rotor, the flow of fibers must become a yarn. The fibers are transmitted through the air channel and begin to move to the tuft state under the influence of centrifugal force in the rotor shaft. As a result of inserting the yarn into the rotor, the fiber tufts start to form a continuous yarn, and the yarn is slowly pulled out and transferred to the bobbin.

High productivity is achieved due to the high-speed movement of working bodies in rotor-spinning machines. Rotor-spun yarn is smoother, more porous, cleaner, and more elastic than ring-spun yarn, so it is widely used in the production of various textile products. Rotor-spinning machines are divided into chamber, rotor, and condenser types. Chamber spinning machines are used to make a wide range of yarns from natural and chemical fibers, while rotor spinning machines are used to spin coarse yarns from low-grade cotton fibers and waste fibers. Condenser spinning machines were mainly used to produce twill yarn using waste fibers, especially flax fiber waste.

The rotor-spinning technique is widely used in the textile industry due to its excellent economic perspective. The rotor is the most important component of the rotor-spinning machine, and its speed has a significant impact on the yarn quality. In the study of Chen and Slater [4], the flow behavior in the rotor changes significantly with the increase in speed. Kocyo and Lawrence [5] conducted studies on twisting mechanics and rotor spinning under different operating conditions. Effect of rotor speed and geometrical parameters on airflow Xiao et al. analyzed by [6] and they found that the angular velocity and slip angle, the good axisymmetry of the spiral structure in the meridional plane of the rotor is achieved.

Some studies have been done on the airflow in the rotor-spinning machine's confusor. Lawrence and Chen [7, 8] used a high-speed camera to capture the fiber morphology during fiber transmission and optimized the design of the confounder combined with an empirical formula. Kong and Platfoot [9, 10] found that changing the geometric dimensions of the confusor or the speed of the opening roller affects the shape of the airflow in the confusor. The airflow then changes the configuration of the fibers flowing inside the channel. They also studied the effect of rotating zones on the fiber configuration during transmission within the channel. Lin et al. [11] investigated the influence of the geometric parameters of the confusor and the spatial position between the rotor and the channel on the characteristics of the airflow in a rotor-spinning machine.

2 Methods

The entire experiment is reduced to measuring force and measuring flow rate, where the flow rate is averaged. The research consists of determining the coefficient of direct (frontal) resistance S_x, researching the pulling action of cotton fibers, and the effect of density. At the same time, two types of channel shapes were chosen for blowing fibers:

- rectangular channel;
- narrowing channel (confusor type)

Which of the selected channels is the most suitable for the transportation of cotton fibers was compared.

Before the start of the experiments, the uniformity and stability of the velocity field of each channel were checked for blowing fibers in an aerodynamic device. Experiments have

shown that the velocity profile in the suspended fiber zone satisfies the conditions of uniformity both in a rectangular channel (Fig. 1a) and in a narrow channel (Fig. 1b).

The airflow speed was varied from 5 m/s to 30 m/s by gradually increasing the fan rotation speed. The measurement range is 30 C. The flow rate was determined using a Pitot tube connected to a micromanometer Benetech GM 8903 Thermoanemometer.

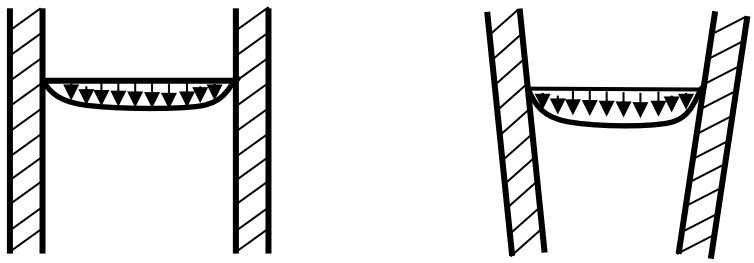

a) *b)*

Fig. 1. The fiber channel located in the confusor. a) – rectangular channel, b) – conical channel.

In the cross-section of the fiber-blowing chamber, the total pressure distribution force was measured using a microtube with an inlet diameter of 6 mm, and the statistical pressure was measured using a statistical pressure tube. At the same time, atmospheric pressure-R_{atm}; ambient temperature -t; and relative humidity-W were measured.

Calculation of the speed of the flow in different sections was carried out by dynamic measurement of dynamic pressure R using a pitot tube, and statistical pressure R according to the static formula [12, 13].

$$V = \xi\sqrt{\frac{2k\sin\alpha(h-h_0)\gamma}{\rho}} \quad (1)$$

here

ξ -The correlation coefficient which is 0.98;
k-equipment calibration coefficient;
α - micromanometer tube liquid slope angle;
ho- the initial indicator of the micromanometer;
ρ- air density, kg/cm^3;
γ- micromanometer liquid density, g/cm^3;

3 Results and discussions

The density value of alcohol was determined with a simple float hydrometer with an accuracy of 0.0001 g/cm^3. The relative deviation of density determination for alcohol ranges from 0.800 to 0.820 g/cm^3 and is equal to

$$\delta_c = \frac{\Delta\gamma}{\gamma} = \frac{0.001}{0.8} = 0.125\% \quad (2)$$

The relative error in determining the angle of inclination of the pipe, including the error in the installation of the crossbar, does not exceed 0.2%, and therefore

$$\delta_c = \frac{\Delta\sin\alpha}{\sin\alpha} \simeq 0.2\% \quad (3)$$

All experiments were performed in triplicate. The required number of measurements was calculated as follows: let δ_s be the systematic error determined by the accuracy class of the instrument or another factor. It is recommended to reduce the random error to such an extent that the error should be less than the systematic one. For this, the value of the absolute error should be smaller than ΔX, δ_s, i.e

$$\Delta\bar{X} \leq \frac{\delta_c}{3}; \quad (4)$$

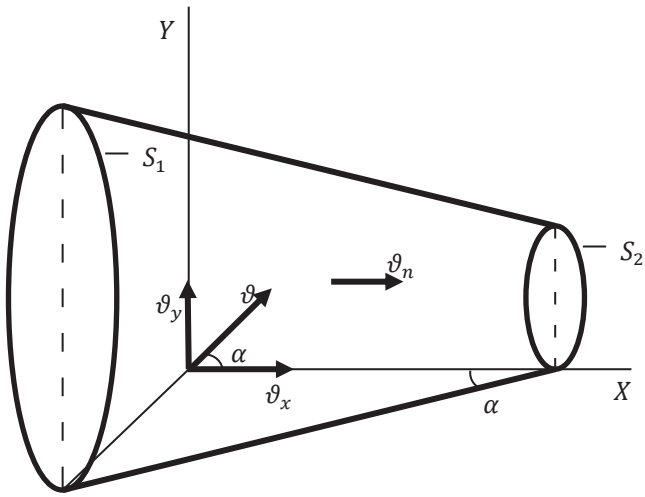

Fig. 2. Channel scheme

Taking into account the air resistance, the following expression (1) was created as a differential equation of motion along the axis OX and OY.

Assuming that the fiber movement channel has a constant cross-section, a coordinate system corresponding to the wall of the fiber movement channel was selected in the axes OX and OY. Taking into account the air resistance, the following expression (1) was created as a differential equation of motion along the axis OX and OY.

$$m \cdot \frac{d\vartheta_y}{dt} = \frac{1}{2} \cdot C_y \cdot S \cdot \rho \cdot \vartheta_y^2 \cdot sin^2\,\alpha$$
$$m \cdot \frac{d\vartheta_x}{dt} = -\frac{1}{2} \cdot C_x \cdot S \cdot \rho \cdot (\vartheta_x^2 \cdot cos^2\,\alpha + \vartheta_n^2) \quad (5)$$

Expression (5) represents the differential equations of the movement of fibers along the channel. Here, (S) are the surfaces through which the fibers flow, C_x and C_y are the resistance coefficients, (ρ) is the air density, and (m) is the mass of the fibers.

$$\frac{dv_y}{v_y^2} = \frac{C_y \rho S \cdot \sin^2\alpha}{2m} \cdot dt$$

In determining the movement of fibers in the conical channel, the total speed was divided into components. When constructing a differential equation of motion, differential equations are integrated, initial and boundary conditions are used, invariant values are found, and general equations of motion are derived.

$$v_y = -\frac{2m}{C_y \rho S \cdot sin^2 \alpha \cdot t} \tag{6}$$

First, the rate of change over time was determined in the differential equation of motion along the *Y*-axis (6).

In determining the rate of change with time in the differential equation of motion along the *Y*-axis, (*m*) the mass of the fiber, (S_y) the resistance coefficient, (*ρ*) the air density, (*S*) the surface of the conical channel, (α) the angle and (*t*) depends on time.

$$Y = -\frac{2m}{C_y \rho S \cdot sin^2 \alpha} \cdot lnt \tag{7}$$

By differentiating the obtained equation (6) concerning time, the equation of the movement trajectory of fibers along *Y* was derived (7). Here (*m*) is the fiber mass, (S_y) the resistance coefficient, (*ρ*) the air density, (*S*) the different surfaces of the conical channel, (*α*) the angle, and (*t*) the time.

In the next case, it was observed that the speed of the surfaces changes in different values over time. The motion of fibers in a conical tube is integrated with the differential equation along the *X*-axis. As a result, the speed along the *X*-axis is determined. It depends on (*m*) fiber mass, (S_y) resistance coefficient, (v_x) air velocity, (*S*) different surfaces of the conical channel, (*α*) angle, and (*t*) time.

$$\frac{dv_x}{v_x^2 \cos^2 \alpha + v_n^2} = -\frac{C_x S \rho}{2m} \cdot dt$$

$$\frac{dv_x}{v_x^2 + \left(\frac{v_n}{\cos \alpha}\right)^2} = -\frac{C_x S \rho}{2m} \cdot \cos^2 \alpha \cdot dt$$

$$\frac{\cos \alpha}{v_n} \, arctg \left(\frac{v_x \cdot \cos \alpha}{v_n}\right) = -\frac{C_x S \rho}{2m} \cos^2 \alpha \cdot t$$

$$arctg \left(\frac{v_x}{v_n} \cos \alpha\right) = -\frac{C_x S \rho \cdot v_n \cdot \cos \alpha}{2m} \cdot t$$

$$v_x = -tg \left(\frac{C_x S \rho \cdot v_n \cdot \cos \alpha}{2m} \cdot t\right) \cdot v_n \cdot \cos \alpha \tag{8}$$

By differentiating the obtained equation (8) by time, the equation of the movement trajectory of the fibers along the *X*-axis (9) was obtained. It depends on (*m*) fiber mass, (S_y) resistance coefficient, (*ρ*) air density, (v_n) velocity, (*S*) different surfaces of the conical channel, (*α*) angle and (*t*) time.

$$x = ln \left(cos \left(\frac{C_x S \rho \cdot v_n \cdot \cos \alpha \cdot t}{2m}\right)\right) \cdot v_n \cdot \cos \alpha \cdot \left(\frac{2m}{C_x S \rho \cdot v_n \cdot \cos \alpha \cdot t}\right)$$

$$x = ln \left(cos \left(\frac{C_x S \rho \cdot v_n \cdot \cos \alpha \cdot t}{2m}\right)\right) \cdot \left(\frac{2m}{C_x S \rho \cdot t}\right) \tag{9}$$

Equations for the dependence of breaking force on speeds are derived.

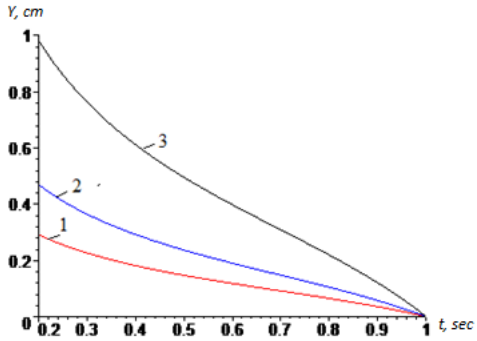

Fig. 3. Time-dependent graph of the movement of fibers in a conical channel along the OY axis on different surfaces $S_1=19.6$, $S_2=12,6$, and $S_3=7.1$.

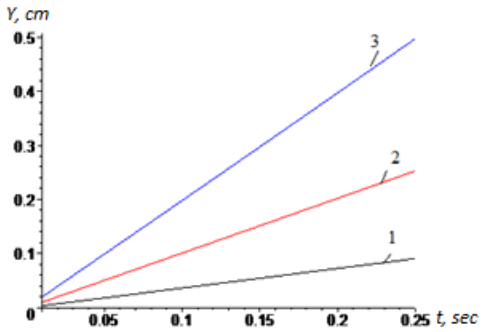

Fig. 4. Time-dependent graph of the movement of fibers in a conical channel along the OY axis at different speeds of $\vartheta_1 = 30m/s$, $\vartheta_2 = 25m/s$, and $\vartheta_3 = 20\ m/s$

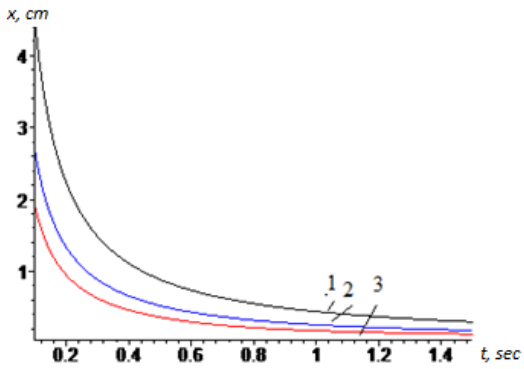

Fig. 5. Time-dependent graph of the movement of fibers in a conical channel along the OX axis on different surfaces $S_1=19.6$, $S_2=12,6$, and $S_3=7.1$.

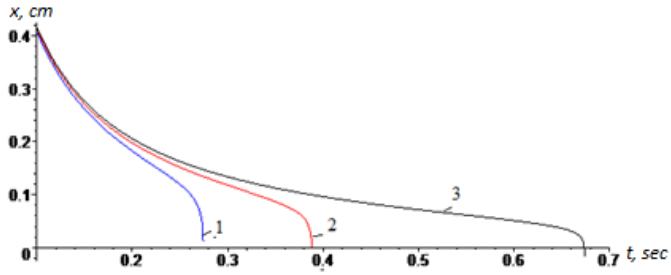

Fig. 6. Time-dependent graph of the movement of fibers along the OX axis in a conical channel at different speeds of ϑ_1 =*30m/s,* ϑ_2 =*25m/s,* and ϑ_3 =*20 m/s.*

4 Conclusions

In the research work, the movement of fibers in the air channel and the rotor in the rotor-spinning machine was studied. In the experimental work, the uniformity and stability of the velocity field of each channel for moving fibers in an aerodynamic device were checked. In this case, the airflow speed was changed from 5 m/s to 30 m/s. Differential equations of motion along the *OX* and *OY*-axis were created taking into account the air resistance. When determining the movement of fibers in a conical channel, the total speed was divided into components, constant values were found, and general equations of motion were derived. Also, the time-dependent graph of the movement of fibers along the *OY*-axis on different surfaces, the time-dependent graph of the movement along the *OY*-axis at different speeds, the movement of fibers along the *OX*-axis in the conical channel time-dependent graphs on different surfaces, time-dependent graphs of movement along the *OX*-axis at different speeds were obtained. The results of the study showed that when the time-dependent graph of the movement of the fibers in the conical channel along the *OY*-axis was obtained on different surfaces S_1=*14,51,* S_2=*12,56,* S_3=*10,75*, the fibers on the small surface were straight. When the velocity is high, the time-dependent graph of the speed of $\boldsymbol{\vartheta_1}$ =*30m/s,* $\boldsymbol{\vartheta_2}$ =*25m/s,* and $\boldsymbol{\vartheta_3}$ =*20 m/s* in the channel was obtained at high speed. Also, when the movement of the fibers in the conical channel along the *OX*-axis is taken as a function of time on different surfaces S_1=*14,51,* S_2=*12,56,*and S_3=*10,75*, the fiber alignment is higher on the small surface, a good result was obtained at high speed when taking the time-dependent graph of the speed of $\boldsymbol{\vartheta_1}$ =*30m/s,* $\boldsymbol{\vartheta_2}$ =*25m/s,* and $\boldsymbol{\vartheta_3}$ =*20 m/s* in the channel.

References

1. Sherzod Korabayev, Jamoliddin Ergashev, Umarjon Meliboyev, Abbosbek Mukhtarov, *AIP Conf. Proc.***2789 (1)**, 040130 (2023)
2. Sh. Korabayev, et al., Scientific and Technical journal of Namangan Institute of Engineering and Technology **8(2)**, 18-22 (2023)
3. Slobodan Stefanovic, Sherzod Korabayev, Sanjar Tojimirzaev, AIP Conf. Proc. **2789(1)**, 040017 (2023)
4. R.H. Chen and K. Slater, J Text Inst **85**: 191–197, (1994)
5. E. Koc¸ and C.A. Lawrence, J Text Inst **97**, 483–492, (2006)
6. M.N. Xiao, H.S. Dou, C.Y. Wu, et al., J Text Res **35**, 136–141 (2014)
7. C.A. Lawrence and K.Z. Chen, J Text Inst **79**, 367–392 (1986)
8. C.A. Lawrence and K.Z. Chen, J Text Inst **79**, 393–408 (1986)
9. L.X. Kong and R.A. Platfoot, Text Res J **66**, 641–650, (1996)
10. L.X. Kong and R.A. Platfoot, Comput Struct **78**, 237–245, (2000)

11. H.T. Lin, J. Wang and Y.C. Zeng, J Text Res **36**, 98–104 (2015)
12. Jakhongir Soloxiddinov, Husanhon Bobojanov, Shavkat Fayzullayev, Sherzod Korabayev, AIP Conf. Proc. **2432 (1)**, 030038 (2022)
13. Jahongir Soloxiddinov, Sherzod Korabayev, Husanhon Bobojanov, Muxayyo Niyazalieva, Xasanboy Ergashev, AIP Conf. **2789 (1)**, 040115 (2023)